

Robustness of spin filtering against current leakage in a Rashba-Dresselhaus-Aharonov-Bohm interferometer

Shlomi Matityahu,¹ Amnon Aharony,^{1,2,3,*} Ora Entin-Wohlman,^{1,2,3} and Shingo Katsumoto⁴

¹*Department of Physics, Ben-Gurion University, Beer Sheva 84105, Israel*

²*Ilse Katz Center for Meso- and Nano-Scale Science and Technology,
Ben-Gurion University, Beer Sheva 84105, Israel*

³*Raymond and Beverly Sackler School of Physics and Astronomy, Tel Aviv University, Tel Aviv 69978, Israel*

⁴*Institute for Solid State Physics, University of Tokyo, Kashiwa, Chiba 277-8581, Japan*

(Dated: October 8, 2018)

In an earlier paper [Phys. Rev. B **84**, 035323 (2011)], we proposed a spin filter which was based on a diamond-like interferometer, subject to both an Aharonov-Bohm flux and (Rashba and Dresselhaus) spin-orbit interactions. Here we show that the full polarization of the outgoing electron spins remains the same even when one allows leakage of electrons from the branches of the interferometer. Once the gate voltage on one of the branches is tuned to achieve an effective symmetry between them, this polarization can be controlled by the electric and/or magnetic fields which determine the spin-orbit interaction strength and the Aharonov-Bohm flux.

PACS numbers: 85.75.Hh, 75.76.+j, 72.25.Dc, 75.70.Tj

Keywords: Spin filter; mobile qubits; spin polarized transport; Rashba and Dresselhaus spin-orbit interactions; Aharonov-Bohm flux; quantum interference devices; tight-binding model.

I. INTRODUCTION

Conventional technology usually exploits the electric charge of the electron. In the last two decades, a new technology has emerged called spintronics, which involves the active control and manipulation of the spin degree of freedom in condensed matter devices.¹⁻³ Adding the spin degree of freedom to the conventional charge-based technology has the potential advantages of multifunctionality, longer decoherence times and lengths, increased data processing speed, decreased electric power consumption, and increased integration densities compared with conventional semiconductor devices. Besides being useful in contemporary technology, spintronics may also contribute to the field of quantum computation and quantum information.⁴ Spin-1/2 is a natural candidate for the quantum bit (qubit) realization. In a spin-based quantum computer, the information is contained in the unit vector along which the spin is polarized. Writing and reading information on a spin qubit is thus equivalent to polarizing the spin along a specific direction and identifying the direction along which the spin is polarized, respectively. We distinguish between two different realizations of spin qubits, namely static and mobile qubits. In static qubit realizations the information transfer is accomplished by transferring the state of the qubit, rather than the qubit itself. For instance, if the qubits are represented by the spins of electrons localized on a quantum dot,⁵⁻⁷ then the information is transferred along a chain of quantum dots via exchange interactions between neighboring dots. With mobile qubits,^{8,9} the qubit itself is moved around the quantum circuit, carrying the information from one point to another. A major advantage of those over static ones is the ability to manipulate mobile qubits by static electric and magnetic fields in pre-defined regions rather than by expensive high-frequency

electromagnetic pulses.¹⁰ Here we consider mobile qubits. In Ref. 8 it has been proposed to implement a system of mobile spin qubits in a two-dimensional electron gas (2DEG) by using surface acoustic waves (SAW) that capture single electrons in their potential minima and drag them through a parallel connection of N quantum one-dimensional channels. A single quantum computation is performed by the N electrons in a single SAW minimum as they are being dragged through a pattern of magnetic and nonmagnetic quantum gates. The feasibility of this setup was demonstrated for two parallel channels ($N = 2$) by Ebbecke *et al.*¹¹

For a quantum computation it is necessary to provide qubits in pure states.⁴ Hence, a major aim of spintronics is to build mesoscopic spin valves (or spin filters), which polarize the spins going through them along tunable directions. At first glance, the easiest way to construct such devices is by using ferromagnets that inject and/or collect polarized electrons. However, the connection of ferromagnets to semiconductors is inefficient, due to a large impedance mismatch between them.^{2,12} A completely different approach is to use spintronic devices that do not involve ferromagnetism at all.^{13,14} Here we discuss such filters that avoid ferromagnets.

Recently, several groups proposed spin filters based on a single loop, subject to both electric and magnetic fields perpendicular to the plane of the loop.¹⁵⁻¹⁷ An important question that has not been addressed in those studies is whether spin filtering is robust against current leakage, for example due to quantum tunnelling out of the loop. Furthermore, in a practical device, with the application of finite source-drain bias voltage, the wires which connect the four dots are inevitably charged up if they are electrostatically isolated. To avoid such probably unfavorable effects, one needs to ground them, which leads to current leakage. In this paper we examine this ques-

tion in the context of the diamond loop subject to both an Aharonov-Bohm (AB) flux¹⁸ and a spin-orbit interaction (SOI), discussed in our previous paper (see Fig. 1).¹⁷ There, we have shown that with a certain symmetry between the two branches of the diamond, and with appropriate tuning of the electric and magnetic fields (or of the diamond shape), this device serves as a perfect spin filter as well as a spin analyzer.

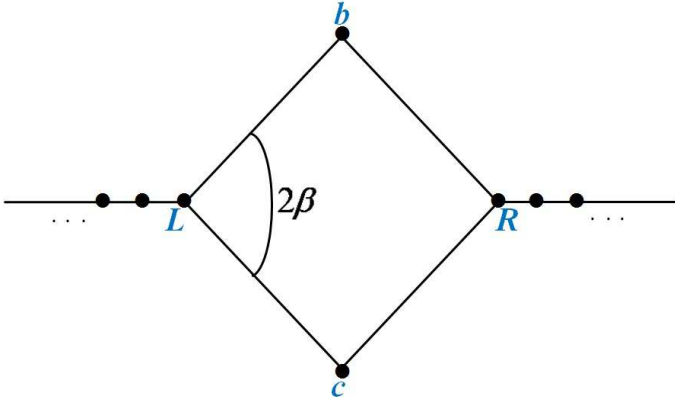


FIG. 1: The lossless diamond. The diamond is penetrated by a magnetic flux Φ , and its edges (of length L) are subject to spin-orbit interactions.

In the presence of an electric field, free electrons experience the well-known SOI in vacuum,¹⁹

$$\mathcal{H}_{SO} = \Lambda \boldsymbol{\sigma} \cdot [\mathbf{p} \times \nabla V(\mathbf{r})]. \quad (1)$$

Here, $\Lambda = \hbar/(2m_0c)^2$ (m_0 is the mass of a free electron and c is the speed of light in vacuum), \mathbf{p} is the electron momentum, $V(\mathbf{r})$ is the electric scalar potential, and the Pauli matrices $\boldsymbol{\sigma}$ are related to the electron spin via $\mathbf{s} = \hbar \boldsymbol{\sigma}/2$. In a 2DEG formed in mesoscopic structures, made of narrow-gap semiconductor heterostructures, the SOI is modified due to an external applied potential (e.g. gate voltage) and a periodic lattice potential.²⁰ The final result can often be recast as an effective SOI Hamiltonian, of the general form $\mathcal{H}_{SO} = (\hbar k_{SO}/m)(\boldsymbol{\pi} \cdot \boldsymbol{\sigma})$, where k_{SO} characterizes the SOI strength, $\boldsymbol{\pi}$ is a linear combination of the electron momentum components p_x and p_y and m is the effective mass, usually much smaller than m_0 . The related energy scale can be larger than that of Eq. (1) by as much as six orders of magnitude.

Two special cases of the linear (in the momentum) SOI should be emphasized, namely the Rashba SOI²¹ and the Dresselhaus SOI.²² The Rashba SOI is a result of a confining potential well which is asymmetric under space inversion. For an electric field $\mathbf{E} = -\nabla V$ in the z direction, this SOI has the form

$$\mathcal{H}_R = \frac{\hbar k_R}{m} (p_y \sigma_x - p_x \sigma_y). \quad (2)$$

The coefficient k_R depends on the magnitude of \mathbf{E} , and can be controlled by a gate voltage, as shown in several experiments.²³⁻²⁷ The Dresselhaus SOI results from

a lattice potential which lacks inversion symmetry. For a 2DEG this SOI is given by

$$\mathcal{H}_D = \frac{\hbar k_D}{m} (p_x \sigma_x - p_y \sigma_y), \quad (3)$$

where k_D usually depends on the crystal structure and only weakly (if at all) on the external field. When a spin moves in the presence of these SOIs a distance L in the direction of the unit vector $\hat{\mathbf{g}}$, its spinor $|\chi\rangle$ transforms into $|\chi'\rangle = U|\chi\rangle$, with the unitary spin rotation matrix $U = e^{i\mathbf{K} \cdot \boldsymbol{\sigma}}$.^{28,29} Here, the vector \mathbf{K} is

$$\mathbf{K} = \alpha_R (-g_y, g_x, 0) + \alpha_D (-g_x, g_y, 0), \quad (4)$$

with the dimensionless coefficients $\alpha_{R,D} \equiv k_{R,D}L$. Below we use the unitary matrix U and the parameters $\alpha_{R,D}$ to characterize the hopping between adjacent bonds in the presence of SOI.

In addition to the SOI related phase, electrons also gain an AB phase ϕ in the presence of a magnetic flux Φ penetrating the loop.¹⁸ When an electron goes around a loop, its wave function gains an AB phase $\phi \equiv 2\pi\Phi/\Phi_0$, where $\Phi_0 = hc/e$ is the flux quantum (e is the electron charge).³⁰ The combined effect of the SOI and the AB flux is to transform the spinor $|\chi\rangle$ of an electron that goes around a loop into $|\chi'\rangle = u|\chi\rangle$, where the unitary matrix u is of the form

$$u = u_{AB} u_{SOI} = e^{i\phi + i\boldsymbol{\omega} \cdot \boldsymbol{\sigma}}. \quad (5)$$

Here $u_{AB} = e^{i\phi} \mathbf{1}$ ($\mathbf{1}$ is the 2×2 unit matrix) is the diagonal transformation matrix due to the AB flux and $u_{SOI} = e^{i\boldsymbol{\omega} \cdot \boldsymbol{\sigma}}$ is the transformation matrix due to the SOI. The latter is a product of matrices of the form $e^{i\mathbf{K} \cdot \boldsymbol{\sigma}}$ discussed above, each coming from the local SOI on a segment of the loop.¹⁷

In the present paper we study the sensitivity of the spin filter to leakage of currents from the branches of the interferometer. To model this leakage, we generalize the diamond interferometer shown in Fig. 1 by allowing for an arbitrary number of tight-binding sites along each edge of the diamond. Each site is connected to a one-dimensional lead, which allows only an outgoing current to an absorbing reservoir (see Fig. 2 and a detailed description below).³¹ We calculate the spin-dependent transmission through the diamond and thus generalize the results of Ref. 17 to include the effects of the leakage. We show that the diamond interferometer may still serve as a perfect spin filter and spin analyzer, even in the presence of current leakage. With slight modifications, the requirements for the symmetry between the two branches and for a specific relation between the AB flux and the SOI strength, derived in Ref. 17, are preserved. There we presented conditions for achieving this symmetry independent of the electrons' energy. These conditions were quite difficult to be realized. Here we show that under linear-response conditions, when all the electrons have the same Fermi energy, it is relatively easy

to achieve this symmetry by tuning a single gate voltage on one of the interferometer branches. Furthermore, we show that once the filtering conditions are obeyed, the blocked polarization and the polarization of the outgoing electrons are not affected by the current leakage, being the same as for the lossless diamond.

The outline of the paper is as follows: in Sec. II we first define the model and present a general calculation of the transmission through the diamond, valid for any internal structure of the two one-dimensional paths (Sec. II A), and then find the conditions for full filtering (Sec. II B). The differences and similarities between the lossless and lossy diamonds are analyzed. The results are discussed and summarized in Sec. III.

II. THE LOSSY DIAMOND

A. Details of the model

Let us consider the scattering of spin-1/2 electrons by a lossy diamond with arbitrary SOI and AB flux, as shown in Fig. 2. Each edge uv ($uv = Lb, Lc, cR, bR$) of the diamond consists of $M + 1$ tight-binding sites with lattice constant a , labelled from left to right. The length of each edge is $L = Ma$ and we allow for arbitrary opening angle, 2β of the diamond. The sites on the corners are labelled as L , R , b and c (Fig. 2) and are characterized by site energies $\epsilon_{0,L}$, $\epsilon_{0,R}$, $\epsilon_{0,b}$ and $\epsilon_{0,c}$, respectively. The sites $n = 1, \dots, M - 1$ on each edge uv have zero site energies $\epsilon_0 = 0$. To allow for a possible current leakage, each of these sites is connected to an absorbing channel, modelled as a one-dimensional tight-binding chain with site energies $\epsilon_0 = 0$ and free of SOI. Electrons can tunnel out of the interferometer through these absorbing channels. The hopping amplitude on the first bond on each absorbing channel is $J_{x,uv}$, while the other bonds have a hopping amplitude j . The diamond is connected at sites L and R to two leads with site energies $\epsilon_0 = 0$ and hopping amplitudes j .

The tight-binding Schrödinger equations for the spinors $|\psi_n^{uv}\rangle$ at sites $n = 1, \dots, M - 1$ on edge uv of the diamond are

$$\epsilon|\psi_n^{uv}\rangle = -J_{uv}(U_{uv}|\psi_{n-1}^{uv}\rangle + U_{uv}^\dagger|\psi_{n+1}^{uv}\rangle) - J_{x,uv}|\Psi_0^{uv}\rangle, \quad (6)$$

where U_{uv} is a 2×2 unitary matrix, J_{uv} is a hopping amplitude for bonds on edge uv , and $|\Psi_0^{uv}\rangle$ is the spinor at the first site of the absorbing channel, connected to one site on edge uv of the diamond. The corresponding equations for the spinors $|\Psi_n^{uv}\rangle$ at sites $n = 0, 1, \dots$ on each of the absorbing channels are

$$\begin{aligned} \epsilon|\Psi_n^{uv}\rangle &= -j(|\Psi_{n-1}^{uv}\rangle + |\Psi_{n+1}^{uv}\rangle), \quad n \geq 1, \\ \epsilon|\Psi_0^{uv}\rangle &= -j|\Psi_1^{uv}\rangle - J_{x,uv}^*|\psi_n^{uv}\rangle. \end{aligned} \quad (7)$$

Assuming only outgoing waves on the absorbing channels, with spinors $|\Psi_n^{uv}\rangle = t_{uv}|\chi^{uv}\rangle e^{ikna}$, and energy

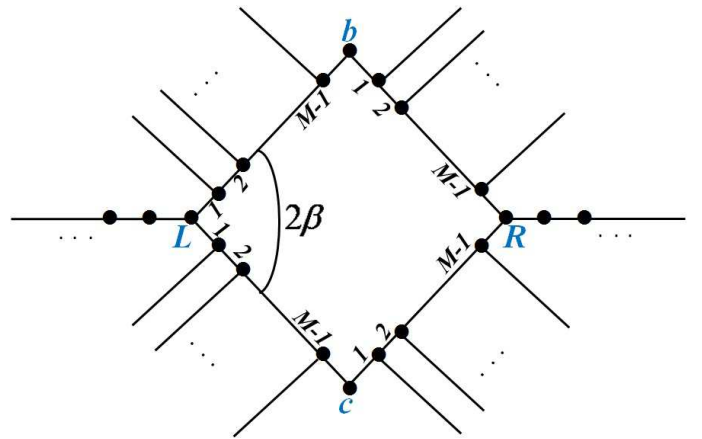


FIG. 2: The lossy diamond. The diamond is penetrated by a magnetic flux Φ , and its edges (of length L) are subject to spin-orbit interaction. Electrons can tunnel out of the interferometer from sites $n = 1, \dots, M - 1$ on edge uv ($uv = Lb, Lc, cR, bR$) through absorbing channels.

$\epsilon = -2j \cos(ka)$, one can eliminate the spinor $|\Psi_0^{uv}\rangle = t_{uv}|\chi^{uv}\rangle$ from Eqs. (7).³¹ Substitution into Eqs. (6) yields

$$(\epsilon - \tilde{\epsilon}_{uv})|\psi_n^{uv}\rangle = -J_{uv}(U_{uv}|\psi_{n-1}^{uv}\rangle + U_{uv}^\dagger|\psi_{n+1}^{uv}\rangle), \quad (8)$$

with the site self energy $\tilde{\epsilon}_{uv}$ given by

$$\tilde{\epsilon}_{uv} = -\frac{|J_{x,uv}|^2 e^{ika}}{j}. \quad (9)$$

The tight-binding Schrödinger equations (8) are easily solved with the transformation

$$|\psi_n^{uv}\rangle = U_{uv}^n|\varphi_n^{uv}\rangle, \quad (10)$$

by which Eqs. (8) read

$$(\epsilon - \tilde{\epsilon}_{uv})|\varphi_n^{uv}\rangle = -J_{uv}(|\varphi_{n-1}^{uv}\rangle + |\varphi_{n+1}^{uv}\rangle). \quad (11)$$

Therefore, in terms of the transformed spinors $|\varphi_n^{uv}\rangle$, the tight-binding equations (11) include neither the AB flux nor the SOI. The solution in terms of the spinors at the diamond corners is thus³²

$$|\varphi_n^{uv}\rangle = \frac{\sin[k_{uv}(M-n)a]|\psi_u\rangle + \sin(k_{uv}na)U_{uv}^{-M}|\psi_v\rangle}{\sin(k_{uv}Ma)}, \quad (12)$$

where the wave vector k_{uv} satisfies the equation

$$\epsilon - \tilde{\epsilon}_{uv} = -2J_{uv} \cos(k_{uv}a). \quad (13)$$

For $J_{x,uv} \neq 0$ the solution of Eq. (13) yields a complex wave vector, which implies an exponential decay of the propagating waves, due to a leakage of part of the electrons out of the interferometer into the absorbing channels.

The tight-binding Schrödinger equations for the spinors at the diamond corners are

$$\begin{aligned} (\epsilon - \epsilon_{0,L}) |\psi_L\rangle &= -J_{Lb} U_{Lb}^\dagger |\psi_1^{Lb}\rangle - J_{Lc} U_{Lc}^\dagger |\psi_1^{Lc}\rangle - j |\psi_{-1}^L\rangle, \\ (\epsilon - \epsilon_{0,b}) |\psi_b\rangle &= -J_{bR} U_{bR}^\dagger |\psi_1^{bR}\rangle - J_{Lb} U_{Lb} |\psi_{M-1}^{Lb}\rangle, \\ (\epsilon - \epsilon_{0,c}) |\psi_c\rangle &= -J_{cR} U_{cR}^\dagger |\psi_1^{cR}\rangle - J_{Lc} U_{Lc} |\psi_{M-1}^{Lc}\rangle, \\ (\epsilon - \epsilon_{0,R}) |\psi_R\rangle &= -J_{cR} U_{cR} |\psi_{M-1}^{cR}\rangle - J_{bR} U_{bR} |\psi_{M-1}^{bR}\rangle \\ &\quad - j |\psi_{M+1}^R\rangle, \end{aligned} \quad (14)$$

with $|\psi_n^L\rangle$ ($n \leq 0$) and $|\psi_n^R\rangle$ ($n \geq M$) being the spinors at the sites on the left and right leads, respectively. By using the transformation (10) together with Eq. (12) for the transformed spinors, Eqs. (14) take the form

$$\begin{aligned} (\epsilon - \epsilon_L) |\psi_L\rangle &= -J_{Lb}'' U_{Lb}^{-M} |\psi_b\rangle - J_{Lc}'' U_{Lc}^{-M} |\psi_c\rangle - j |\psi_{-1}^L\rangle, \\ (\epsilon - \epsilon_b) |\psi_b\rangle &= -J_{bR}'' U_{bR}^{-M} |\psi_R\rangle - J_{Lb}'' U_{Lb}^M |\psi_L\rangle, \\ (\epsilon - \epsilon_c) |\psi_c\rangle &= -J_{cR}'' U_{cR}^{-M} |\psi_R\rangle - J_{Lc}'' U_{Lc}^M |\psi_L\rangle, \\ (\epsilon - \epsilon_R) |\psi_R\rangle &= -J_{cR}'' U_{cR}^M |\psi_c\rangle - J_{bR}'' U_{bR}^M |\psi_b\rangle \\ &\quad - j |\psi_{M+1}^R\rangle, \end{aligned} \quad (15)$$

with the site self energies

$$\begin{aligned} \epsilon_L &= \epsilon_{0,L} - J'_{Lb} - J'_{Lc}, \\ \epsilon_b &= \epsilon_{0,b} - J'_{bR} - J'_{Lb}, \\ \epsilon_c &= \epsilon_{0,c} - J'_{Lc} - J'_{cR}, \\ \epsilon_R &= \epsilon_{0,R} - J'_{cR} - J'_{bR}, \end{aligned} \quad (16)$$

and with

$$J'_{uv} = J_{uv} \frac{\sin [k_{uv} (M-1) a]}{\sin (k_{uv} Ma)}, \quad (17)$$

$$J''_{uv} = J_{uv} \frac{\sin (k_{uv} a)}{\sin (k_{uv} Ma)}. \quad (18)$$

Equations (15) are analogous to Eqs. (7) of Ref. 17. All the modifications caused by the current leakage are embodied in the site self energies ϵ_L , ϵ_b , ϵ_c , and ϵ_R [Eqs. (16) and (17)] and the complex effective hopping amplitudes J''_{Lb} , J''_{Lc} , J''_{cR} , J''_{bR} [Eqs. (18)].³³ Elimination of $|\psi_b\rangle$ and $|\psi_c\rangle$ from Eqs. (15) yields

$$\begin{aligned} (\epsilon - y_L) |\psi_L\rangle &= \mathbf{W}_{RL} |\psi_R\rangle - j |\psi_{-1}^L\rangle, \\ (\epsilon - y_R) |\psi_R\rangle &= \mathbf{W}_{LR} |\psi_L\rangle - j |\psi_{M+1}^R\rangle, \end{aligned} \quad (19)$$

where

$$\begin{aligned} y_L &= \epsilon_L + \frac{J''_{Lb}^2}{\epsilon - \epsilon_b} + \frac{J''_{Lc}^2}{\epsilon - \epsilon_c}, \\ y_R &= \epsilon_R + \frac{J''_{bR}^2}{\epsilon - \epsilon_b} + \frac{J''_{cR}^2}{\epsilon - \epsilon_c}, \end{aligned} \quad (20)$$

$$\begin{aligned} \mathbf{W}_{LR} &= \gamma_b U_b + \gamma_c U_c, \\ \mathbf{W}_{RL} &= \gamma_b U_b^\dagger + \gamma_c U_c^\dagger, \end{aligned} \quad (21)$$

with the complex coefficients

$$\begin{aligned} \gamma_b &= \frac{J''_{Lb} J''_{bR}}{\epsilon - \epsilon_b}, \\ \gamma_c &= \frac{J''_{Lc} J''_{cR}}{\epsilon - \epsilon_c}, \end{aligned} \quad (22)$$

and the unitary matrices

$$\begin{aligned} U_b &= U_{bR}^M U_{Lb}^M, \\ U_c &= U_{cR}^M U_{Lc}^M. \end{aligned} \quad (23)$$

The matrices U_b and U_c correspond to transitions from left to right through the upper and lower paths, respectively.

Consider a wave coming from the left, namely

$$\begin{aligned} |\psi_n^L\rangle &= |\chi_{in}\rangle e^{ikna} + r |\chi_r\rangle e^{-ikna}, & n \leq 0, \\ |\psi_n^R\rangle &= t |\chi_t\rangle e^{ik(n-M)a}, & n \geq M, \end{aligned} \quad (24)$$

where $|\chi_{in}\rangle$, $|\chi_r\rangle$ and $|\chi_t\rangle$ are the incoming, reflected and transmitted normalized spinors, respectively, with the corresponding reflection and transmission amplitudes r and t . The transmission and reflection amplitude matrices are defined by the relations

$$t |\chi_t\rangle \equiv \mathcal{T} |\chi_{in}\rangle, \quad r |\chi_r\rangle \equiv \mathcal{R} |\chi_{in}\rangle. \quad (25)$$

To calculate these matrices, we substitute Eqs. (24) into Eqs. (19). This yields¹⁷

$$\mathcal{T} = 2ij \sin(ka) \mathbf{W}_{LR} (Y \mathbf{1} - \mathbf{W}_{RL} \mathbf{W}_{LR})^{-1}, \quad (26)$$

$$\mathcal{R} = -\mathbf{1} - 2ij \sin(ka) X_R (Y \mathbf{1} - \mathbf{W}_{RL} \mathbf{W}_{LR})^{-1}, \quad (27)$$

where

$$\begin{aligned} X_{L,R} &= y_{L,R} + j e^{-ika}, \\ Y &= X_L X_R. \end{aligned} \quad (28)$$

Compared with the expressions for the transmission and reflection amplitudes of the lossless diamond [Eqs. (14) in Ref. 17], one notes the following difference. In the lossless diamond the coefficients γ_b and γ_c [Eqs. (22)] are real and then, according to Eqs. (21), the relation $\mathbf{W}_{RL} = \mathbf{W}_{LR}^\dagger$ holds. In the lossy diamond, on the other hand, the coefficients γ_b and γ_c are complex and $\mathbf{W}_{RL} \neq \mathbf{W}_{LR}^\dagger$. Hence $\mathbf{W}_{RL} \mathbf{W}_{LR}$, involved in both \mathcal{T} and \mathcal{R} , is not an hermitian matrix as in the lossless case. Nevertheless, in the next subsection we show that spin filtering may still be obtained in the presence of current leakage by appropriately tuning the gate voltages and the magnetic field.

B. Filtering conditions for the lossy diamond

In this section we study the properties of the spin-dependent transmission matrix (26) and write it in a form

that enables us to derive the spin filtering conditions. Consider first the matrix $\mathbf{W}_{RL}\mathbf{W}_{LR}$. Using Eqs. (21), we get

$$\mathbf{W}_{RL}\mathbf{W}_{LR} = \gamma_b^2 + \gamma_c^2 + \gamma_b\gamma_c(u + u^\dagger), \quad (29)$$

where $u = U_b^\dagger U_c$ is the unitary matrix representing an anticlockwise hopping from site L back to site L around the loop. As discussed in the introduction, the matrix u has the form $u = e^{i\phi+i\omega\cdot\sigma}$ and therefore $u + u^\dagger = 2(\cos\omega\cos\phi - \sin\omega\sin\phi\hat{\omega}\cdot\sigma)$. Thus, Eq. (29) can be written as

$$\mathbf{W}_{RL}\mathbf{W}_{LR} = A + \mathbf{B} \cdot \boldsymbol{\sigma}, \quad (30)$$

with

$$\begin{aligned} A &= \gamma_b^2 + \gamma_c^2 + 2\gamma_b\gamma_c \cos\omega\cos\phi, \\ \mathbf{B} &= 2\gamma_b\gamma_c \sin\omega\sin\phi \hat{\mathbf{n}} = B\hat{\mathbf{n}}. \end{aligned} \quad (31)$$

Here, $\hat{\mathbf{n}} \equiv -\hat{\omega}$ is a real unit vector along the direction of $-\omega$. Defining the eigenstates of the spin component along an arbitrary direction $\hat{\mathbf{n}}$ via $\hat{\mathbf{n}}\cdot\boldsymbol{\sigma}|\pm\hat{\mathbf{n}}\rangle = \pm|\pm\hat{\mathbf{n}}\rangle$, we identify the eigenvectors of $\mathbf{W}_{RL}\mathbf{W}_{LR}$ as $|\pm\hat{\mathbf{n}}\rangle$, namely

$$\mathbf{W}_{RL}\mathbf{W}_{LR}|\pm\hat{\mathbf{n}}\rangle = \lambda_\pm|\pm\hat{\mathbf{n}}\rangle, \quad (32)$$

with the corresponding eigenvalues λ_\pm being

$$\lambda_\pm = A \pm B = \gamma_b^2 + \gamma_c^2 + 2\gamma_b\gamma_c \cos(\phi \pm \omega). \quad (33)$$

Consider an incoming electron with its spin polarized along $\pm\hat{\mathbf{n}}$. The spinor at the output of the diamond will be

$$t_\pm|\chi_\pm^{\text{out}}\rangle = \mathcal{T}|\pm\hat{\mathbf{n}}\rangle = \frac{2ij\sin(ka)}{Y - \lambda_\pm}\mathbf{W}_{LR}|\pm\hat{\mathbf{n}}\rangle. \quad (34)$$

The transmission amplitudes t_\pm for the two opposite polarizations are calculated from the scalar product of Eq. (34) with itself using the normalization condition $\langle\chi_\pm^{\text{out}}|\chi_\pm^{\text{out}}\rangle = 1$. Thus,

$$|t_\pm|^2 = \left| \frac{2ij\sin(ka)}{Y - \lambda_\pm} \right|^2 \langle \pm\hat{\mathbf{n}} | \mathbf{W}_{LR}^\dagger \mathbf{W}_{LR} | \pm\hat{\mathbf{n}} \rangle. \quad (35)$$

To calculate the expectation value in Eq. (35), note that by using Eqs. (21) the matrix $\mathbf{W}_{LR}^\dagger \mathbf{W}_{LR}$ is found to be

$$\mathbf{W}_{LR}^\dagger \mathbf{W}_{LR} = |\gamma_b|^2 + |\gamma_c|^2 + (\gamma_b^* \gamma_c u + \gamma_b \gamma_c^* u^\dagger). \quad (36)$$

Substituting $u = e^{i\phi+i\omega\cdot\sigma}$, $\gamma_b = |\gamma_b|e^{i\delta_b}$ and $\gamma_c = |\gamma_c|e^{i\delta_c}$ into the last relation gives

$$\mathbf{W}_{LR}^\dagger \mathbf{W}_{LR} = A_{LR} + \mathbf{B}_{LR} \cdot \boldsymbol{\sigma}, \quad (37)$$

with

$$\begin{aligned} A_{LR} &= |\gamma_b|^2 + |\gamma_c|^2 + 2|\gamma_b||\gamma_c| \cos\omega\cos\tilde{\phi}, \\ \mathbf{B}_{LR} &= 2|\gamma_b||\gamma_c| \sin\omega\sin\tilde{\phi} \hat{\mathbf{n}} = B_{LR}\hat{\mathbf{n}}, \end{aligned} \quad (38)$$

and $\tilde{\phi} = \phi + \delta_c - \delta_b$. Hence, the eigenvectors of $\mathbf{W}_{LR}^\dagger \mathbf{W}_{LR}$ are also $|\pm\hat{\mathbf{n}}\rangle$ and the corresponding eigenvalues are

$$\begin{aligned} \lambda_{LR,\pm} &= A_{LR} \pm B_{LR} = |\gamma_b|^2 + |\gamma_c|^2 \\ &+ 2|\gamma_b||\gamma_c| \cos(\tilde{\phi} \pm \omega). \end{aligned} \quad (39)$$

Then, according to Eq. (35) the transmission amplitudes t_\pm are

$$|t_\pm| = \frac{2j|\sin(ka)|}{|Y - \lambda_\pm|} \sqrt{\lambda_{LR,\pm}}. \quad (40)$$

Now let us find the direction of the transmitted spinors $|\chi_\pm^{\text{out}}\rangle$. Substituting Eq. (40) into Eq. (34), we get

$$|\chi_\pm^{\text{out}}\rangle = \frac{e^{-i\delta_\pm}}{\sqrt{\lambda_{LR,\pm}}} \mathbf{W}_{LR} |\pm\hat{\mathbf{n}}\rangle, \quad (41)$$

with δ_\pm being some arbitrary phases. Using Eqs. (32) and (41), one finds

$$\mathbf{W}_{LR}\mathbf{W}_{RL}|\chi_\pm^{\text{out}}\rangle = \lambda_\pm|\chi_\pm^{\text{out}}\rangle, \quad (42)$$

which shows that $|\chi_\pm^{\text{out}}\rangle$ is an eigenstate of $\mathbf{W}_{LR}\mathbf{W}_{RL}$. Calculating this matrix from Eqs. (21), we find

$$\mathbf{W}_{LR}\mathbf{W}_{RL} = \gamma_b^2 + \gamma_c^2 + \gamma_b\gamma_c(u' + u'^\dagger), \quad (43)$$

with $u' = U_b U_c^\dagger$. The eigenvectors of the matrix $\mathbf{W}_{LR}\mathbf{W}_{RL}$ correspond to some new direction $\hat{\mathbf{n}}'$, so that $|\chi_\pm^{\text{out}}\rangle = |\pm\hat{\mathbf{n}}'\rangle$. Therefore we can write \mathbf{W}_{LR} as

$$\mathbf{W}_{LR} = e^{i\delta_-} \sqrt{\lambda_{LR,-}} |\hat{\mathbf{n}}'\rangle\langle -\hat{\mathbf{n}}| + e^{i\delta_+} \sqrt{\lambda_{LR,+}} |\hat{\mathbf{n}}'\rangle\langle \hat{\mathbf{n}}|. \quad (44)$$

Similarly, Eq. (34) implies that the transmission amplitude matrix [Eq. (26)] has the form

$$\mathcal{T} = t_-|-\hat{\mathbf{n}}'\rangle\langle -\hat{\mathbf{n}}| + t_+|\hat{\mathbf{n}}'\rangle\langle \hat{\mathbf{n}}|. \quad (45)$$

This form enables us to derive the explicit conditions for spin filtering as follows.

Expanding an arbitrary incoming spinor $|\chi_{\text{in}}\rangle$ in the basis $|\pm\hat{\mathbf{n}}\rangle$,

$$|\chi_{\text{in}}\rangle = c_-|-\hat{\mathbf{n}}\rangle + c_+|\hat{\mathbf{n}}\rangle, \quad (46)$$

where $c_\pm \equiv \langle \pm\hat{\mathbf{n}} | \chi_{\text{in}} \rangle$, the outgoing spinor is

$$t|\chi_{\text{out}}\rangle = \mathcal{T}|\chi_{\text{in}}\rangle = c_-t_-|-\hat{\mathbf{n}}\rangle + c_+t_+|\hat{\mathbf{n}}\rangle. \quad (47)$$

Equation (47) implies that the outgoing spinor is polarized along a definite direction $|\mp\hat{\mathbf{n}}'\rangle$, provided that one of the eigenvalues $\lambda_{LR,\pm}$ vanishes. For example, if $\lambda_{LR,-} = 0$, then $t_- = 0$ [Eq. (40)] and the lossy diamond then serves as a perfect spin filter, since all outgoing electrons have their spin polarized along $\hat{\mathbf{n}}'$. Moreover, once the parameters of the device have been appropriately tuned so that $t_- = 0$, this device can also

serve as a spin analyzer.¹⁷ We emphasize that the blocked spinors, $|\pm \hat{n}\rangle$, and the transmitted ones, $|\pm \hat{n}'\rangle$, being the eigenvectors of the matrices $\mathbf{W}_{RL}\mathbf{W}_{LR}$ [Eq. (29)] and $\mathbf{W}_{LR}\mathbf{W}_{RL}$ [Eq. (43)], respectively, are completely determined by the AB and SOI phases. To see this, note that the eigenvectors of $\mathbf{W}_{RL}\mathbf{W}_{LR}$ and $\mathbf{W}_{LR}\mathbf{W}_{RL}$ are simply the eigenvectors of $u + u^\dagger$ and $u' + u'^\dagger$, respectively, where $u = U_b^\dagger U_c = U_{Lb}^{-M} U_{bR}^{-M} U_{cR}^M U_{Lc}^M$ and $u' = U_b U_c^\dagger = U_{bR}^M U_{Lb}^M U_{Lc}^{-M} U_{cR}^{-M}$. Since the hopping matrices U_{uv} depend only on the AB and SOI phases, the directions $\pm \hat{n}$ and $\pm \hat{n}'$ are determined solely by these phases and are not affected by the current leakage. Hence, the blocked and transmitted directions can be manipulated by the external electric and magnetic fields.

From Eq. (39) it follows that $\lambda_{LR,\pm} \geq 0$ and the equality $\lambda_{LR,-} = 0$ holds only if

$$|\gamma_b| = |\gamma_c| \equiv \gamma, \quad \cos(\tilde{\phi} - \omega) = -1. \quad (48)$$

We now discuss these two conditions.

The first condition in Eqs. (48) can be interpreted as a requirement for a symmetry relation between the two paths. Recall that γ_b and γ_c are the complex effective hopping amplitudes for the two branches of the loop. In the case of the lossless diamond, we required that this condition be satisfied independently of the electron energy ϵ . In the present case, this symmetry can be achieved by tuning the various parameters of edges Lb and bR to be equal to those of edges Lc and cR , i.e. either

$$\begin{aligned} J_{Lb} &= J_{Lc}, & J_{bR} &= J_{cR}, \\ J_{x,Lb} &= J_{x,Lc}, & J_{x,bR} &= J_{x,cR}, \end{aligned} \quad (49)$$

or

$$\begin{aligned} J_{Lb} &= J_{cR}, & J_{bR} &= J_{Lc}, \\ J_{x,Lb} &= J_{x,cR}, & J_{x,bR} &= J_{x,Lc}, \end{aligned} \quad (50)$$

and in addition $\epsilon_{0,b} = \epsilon_{0,c}$. However, it is not obvious that such a tuning of the parameters can be realized in an experimental setup.

Alternatively, one can work in the linear-response regime, where all the electrons have the same energy, equal to the Fermi energy of the leads. In this case, the first condition in Eqs. (48) should be satisfied for a single specific energy, and this can be achieved by tuning only a single gate voltage, e.g. that which controls the site energy $\epsilon_{0,b}$ (or $\epsilon_{0,c}$).

The second condition in Eqs. (48), namely $\omega = \tilde{\phi} + \pi$, imposes a relation between the AB flux and the SOI strength. We remind the reader that $\tilde{\phi} = \phi + \delta_c - \delta_b$, with δ_b and δ_c being the phases of γ_b and γ_c , respectively. This should be compared with the condition $\omega = \phi + \pi$, derived for the lossless diamond.¹⁷ As emphasized in Ref.

17, this relation for the lossless diamond depends neither on the electron energy ϵ , nor on the site energies, since ϕ and ω depend only on the unitary matrices U_i . In the lossy diamond, on the other hand, the relation $\omega = \tilde{\phi} + \pi$ generally depends both on the electron energy and on the site energies [since γ_b and γ_c depend on these parameters, see Eqs. (22)]. However, with one of the choices (49) or (50), the two paths are completely symmetric, so that $\delta_b = \delta_c$ and the relation between the AB flux and the SOI strength becomes identical to that of the lossless diamond. Alternatively, working in the linear-response regime, one has to tune experimentally the AB flux to satisfy the condition $\omega = \phi + \delta_c - \delta_b + \pi$ for specific values of δ_b and δ_c (which are determined by the Fermi energy of the leads and by the various hopping amplitudes, site energies and leakage parameters). For further details, see the appendix.

Finally, we comment on the magnitude of the transmission of the polarized electrons through the filter. Since one does not expect the tight-binding model to be valid near the band edges, we confine ourselves to the center of the band, $\epsilon = 0$ or $ka = \pi/2$, where the details of the model chosen are not so important. In the lossless diamond, it was shown in Ref. 17 that by fixing j and $J_{uv} \equiv J$, one has $T_+(\epsilon = 0) = |t_+(\epsilon = 0)|^2 = 1$ at $\phi = \phi_0$ if the various parameters are tuned to be $\gamma = \gamma_0 = j/(2 \sin \phi_0)$, $\epsilon_{0,b} = -J^2/\gamma_0$, and $\epsilon_{0,L} = \epsilon_{0,R} = -2\gamma_0$. Using Eq. (40) with these choices, the transmission $T_+(\epsilon = 0) = |t_+(\epsilon = 0)|^2$ takes the form¹⁷

$$T_+(\epsilon = 0, \phi) = \frac{4 \sin^2 \phi \sin^2 \phi_0}{(\sin^2 \phi + \sin^2 \phi_0)^2}. \quad (51)$$

This function is plotted in Fig. 3(a) for two values of ϕ_0 and for $J = 4j$. To compare with the transmission T_+ of the lossy diamond, we use the same parameters chosen above, but now we "turn on" the leakage by setting $M = 5$ and $J_{x,uv} = 0.2j$. The results are shown in Fig. 3(a). Figure 3(b) shows the transmission T_+ as a function of ka with the AB flux fixed at $\phi = \phi_0$, for the parameters chosen above and for $J = 4j$. Two curves correspond to the lossless diamond ($M = 1$ and $J_{x,uv} = 0$) and the other two correspond to the lossy diamond with $M = 5$ and $J_{x,uv} = 0.2j$. Comparing the transmissions of lossless and the lossy diamonds presented in Fig. 3, several differences can be detected. First, the maximal transmission of the lossy diamond is less than one. This is an obvious effect of the lossy diamond, since part of the incident current leaks into the absorbing channels. This leakage increases as the tunnelling from the diamond edges to each absorbing channel, represented by $J_{x,uv}$, increases or when the number of absorbing channels M increases. Second, Fig. 3(a) shows that the maximal transmission is not obtained for $\phi = \phi_0$ but for a flux slightly larger than ϕ_0 . Third, in Fig. 3(b) we see that the transmission as a function of ka is much narrower than that of the lossless case.

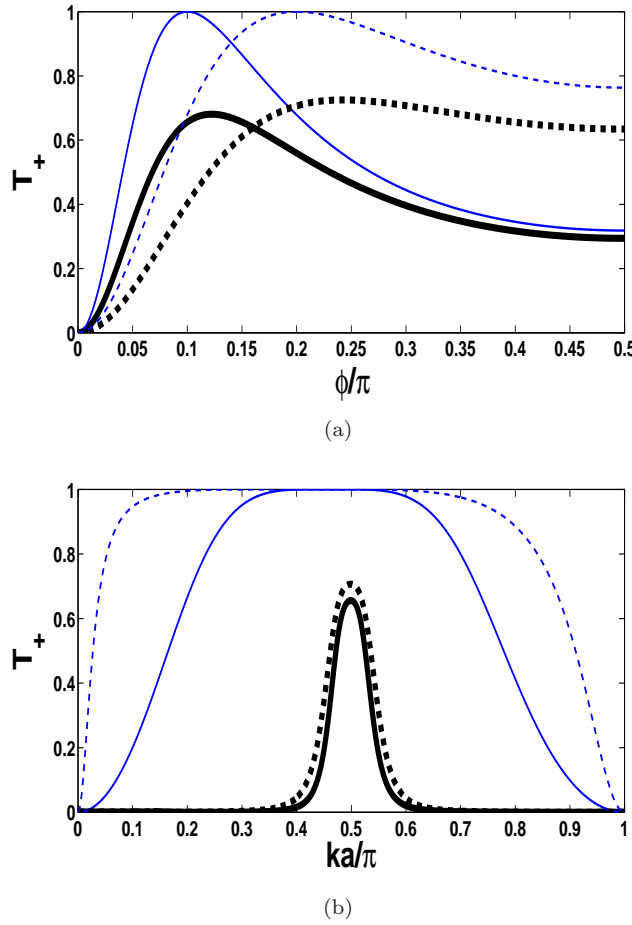


FIG. 3: (Color online) The transmission of the polarized electrons, $T_+(\epsilon, \phi)$ (a) as a function of the AB flux ϕ (in units of π) for $\epsilon = 0$ ($ka = \pi/2$) and (b) as a function of ka (in units of π) for $\phi = \phi_0$. Solid and dashed curves correspond to maxima of $T_+(\epsilon = 0, \phi)$ at $\phi_0 = 0.1\pi$ and $\phi_0 = 0.2\pi$, respectively. Thin (blue) and thick (black) curves correspond to the lossless ($M = 1$ and $J_{x,uv} = 0$) and lossy ($M = 5$ and $J_{x,uv} = 0.2j$) diamonds, respectively.

III. SUMMARY AND CONCLUSIONS

We have generalized the results of the single-diamond interferometer made of materials with significant SOIs and penetrated by an AB flux, discussed in Ref. 17, to the case where losses are present. In particular, we have considered losses due to a current leakage out of the diamond into absorbing channels, modelled as 1D tight-binding chains. Our calculations show that spin filtering (and consequently also spin reading) can be achieved even in the presence of current leakage. The filtering conditions found in Ref. 17, namely the condition for a symmetry relation between the two branches ($\gamma_b = \gamma_c$) and the relation between the AB phase and the SOI phase ($\phi = \omega + \pi$) are modified. In the lossy diamond γ_b and γ_c are complex numbers and the first condition

takes the form $|\gamma_b| = |\gamma_c|$. Since γ_b and γ_c depend on the various parameters (leakage parameters $J_{x,uv}$, hopping amplitudes J_{uv} , electron energy ϵ and site energies $\epsilon_{0,b}$ and $\epsilon_{0,c}$) in a complicated manner, it is difficult to derive general analytical relations between these parameters from this condition. The solution simplifies for the completely symmetric diamond [Eqs. (49) and (50)] for which the condition $|\gamma_b| = |\gamma_c|$ is trivially satisfied. The second condition, $\phi = \omega + \pi$, is still valid provided that ϕ is replaced by $\phi = \phi + \delta_c - \delta_b$, with δ_b and δ_c being the phases of γ_b and γ_c , respectively. For the completely symmetric diamond one has $\delta_b = \delta_c$ and this condition is the same as for the lossless diamond. An alternative way to satisfy the filtering conditions is by working in the linear-response regime. In that regime, transport of electrons occurs at the Fermi energy of the leads. The filtering conditions can then be satisfied simultaneously by tuning the AB flux and one of the site energies $\epsilon_{o,b}$ or $\epsilon_{o,c}$.

Once the filtering conditions are obeyed, the transmitted electrons are fully polarized. The effects of the leakage on the transmission can be summarized as follows:

- (1) The maximal transmission in the lossy diamond is always smaller than one and the maximum decreases with increasing leakage parameters or with increasing length of each edge of the diamond.
- (2) Viewed as a function of the flux ϕ , the transmission of the lossy diamond is shifted to slightly higher fluxes relative to the transmission of the lossless diamond, while viewed as a function of ka , the transmission of the lossy diamond is narrower than the transmission of the lossless diamond.

However, it should be emphasized that quantities which depend only on the hopping matrices U_{uv}^M , are not affected by the leakage. For instance, the dependence of the SOI phase ω on the SOI strength and on the geometry of the diamond (through the opening angle 2β) is the same as in the lossless diamond and so are the directions \hat{n} and \hat{n}' of the filtered and the transmitted electrons. Analytical expressions for the SOI phase and for the blocked and transmitted spinors in the lossless diamond have been obtained in Ref. 17 for the Rashba-only SOI and for both Rashba and Dresselhaus SOI.³⁴ Those expressions thus remain valid for the lossy diamond.

In conclusion, while the filtering conditions are slightly modified, many of the device properties remain the same as in the lossless case. These properties can be manipulated by external electric and magnetic fields and are insensitive to the current leakage in the framework of the model presented here.

Appendix: spin filtering in the asymmetric interferometer

We have pointed out that realizing a symmetric interferometer in the experiment may be a difficult task. We

have mentioned that the filtering conditions (48) can be fulfilled for an arbitrary asymmetric interferometer by working in the linear-response regime. Let us assume that the Fermi energy of the leads lies at the center of the tight-binding band (i.e. $\epsilon = \epsilon_F = 0$ or $ka = \pi/2$). Then, one can satisfy the first condition in Eqs. (48) (with $\epsilon = 0$) by tuning only the site energy $\epsilon_{0,b}$. The phase $\delta_b - \delta_c$ is then fixed, and one can satisfy the second condition in Eqs. (48) by tuning the AB flux. To examine the variation of γ_b/γ_c as a function of $\epsilon_{0,b}$, we set $J_{Lb} = 3j$, $J_{bR} = 4j$, $J_{Lc} = 2.5j$, $J_{cR} = 3.8j$, $J_{x,Lb} = 0.1j$, $J_{x,bR} = 0.2j$, $J_{x,Lc} = 0.05j$, $J_{x,cR} = 0.25j$, $M = 5$ and $\epsilon_{0,c} = 2j$ and plot $|\gamma_b/\gamma_c|$ and $\delta_b - \delta_c$ in Fig. 4 as a function of $\epsilon_{0,b}$. The dashed (red) line in Fig. 4(a) corresponds to $|\gamma_b/\gamma_c| = 1$. The intersection of the two curves occurs at the values $\epsilon_{0,b}^*$ for which the first condition in Eqs. (48) holds. Figure 4(a) shows that $|\gamma_b/\gamma_c|$

changes slowly at the vicinity of $\epsilon_{0,b}^*$. Furthermore, Fig. 4(b) shows that the phase $\delta_b - \delta_c$ is also a slowly varying function of $\epsilon_{0,b}$ at the vicinity of $\epsilon_{0,b}^*$. This means that the fulfillment of the filtering conditions (48) is not sensitive to small deviations of $\epsilon_{0,b}$ from $\epsilon_{0,b}^*$. The results presented in Fig. 4 have a weak dependence on the various energies. The width and the height of the peak in Fig. 4(a) and the width of the crossover region in Fig. 4(b) change slightly with the various energies, but the overall shape is robust.

Acknowledgments

We acknowledge support from the Israel Science Foundation (ISF).

* Electronic address: aaharony@bgu.ac.il

¹ S. A. Wolf, D. D. Awschalom, R. A. Buhrman, J. M. Daughton, S. von Molnár, M. L. Roukes, A. Y. Chtchelkina, and D. M. Treger, *Science* **294**, 1488 (2001).

² I. Žutić, J. Fabian, and S. Das Sarma, *Rev. Mod. Phys.* **76**, 323 (2004).

³ S. D. Bader and S. S. P. Parkin, *Annu. Rev. Condens. Matter Phys.* **1**, 71 (2010).

⁴ M. A. Nielsen and I. L. Chuang, *Quantum Computation and Quantum Information*, (Cambridge University Press, Cambridge, 2011).

⁵ D. Loss and D. P. DiVincenzo, *Phys. Rev. A* **57**, 120 (1998).

⁶ F. L. H. Koppens, C. Buizert, K. J. Tierlooij, I. T. Vink, K. C. Nowack, T. Meunier, L. P. Kouwenhoven, and L. M. K. Vandersypen, *Nature (London)* **442**, 766 (2006).

⁷ M. Pioro-Ladrière, T. Obata, Y. Tokura, Y.-S. Shin, T. Kubo, K. Yoshida, T. Taniyama, and S. Tarucha, *Nat. Phys.* **4**, 776 (2008).

⁸ C. H. W. Barnes, J. M. Shilton, and A. M. Robinson, *Phys. Rev. B* **62**, 8410 (2000).

⁹ A. E. Popescu, and R. Ionicioiu, *Phys. Rev. B* **69**, 245422 (2004).

¹⁰ T. Hayashi, T. Fujisawa, H. D. Cheong, Y. H. Jeong, and Y. Hirayama, *Phys. Rev. Lett.* **91**, 226804 (2003).

¹¹ J. Eberbeck, G. Bastian, M. Blöcker, K. Pierz, and F. J. Ahlers, *Appl. Phys. Lett.* **77**, 2601 (2000).

¹² G. Schmidt, D. Ferrand, L. W. Molenkamp, A. T. Filip, and B. J. Van Wees, *Phys. Rev. B* **62**, R4790 (2000).

¹³ Y. Kato, R. C. Myers, A. C. Gossard, and D. D. Awschalom, *Nature (London)* **427**, 50 (2004).

¹⁴ D. D. Awschalom and N. Samarth, *Physics* **2**, 50 (2009).

¹⁵ R. Citro, F. Romeo, and M. Marinaro, *Phys. Rev. B* **74**, 115329 (2006).

¹⁶ N. Hatano, R. Shirasaki, and H. Nakamura, *Phys. Rev. A* **75**, 032107 (2007).

¹⁷ A. Aharony, Y. Tokura, G. Z. Cohen, O. Entin-Wohlman, and S. Katsumoto, *Phys. Rev. B* **84**, 035323 (2011).

¹⁸ Y. Aharonov and D. Bohm, *Phys. Rev.* **115**, 485 (1959).

¹⁹ J. J. Sakurai, *Modern Quantum Mechanics* (Addison Wesley, Boston, 1994), p. 304.

²⁰ R. Winkler, *Spin-Orbit Coupling Effects in Two-Dimensional Electron and Hole Systems* (Springer-Verlag, Berlin, 2003).

²¹ E. I. Rashba, *Fiz. Tverd. Tela (Leningrad)* **2**, 1224 (1960) [*Sov. Phys. Solid State* **2**, 1109 (1960)]; Y. A. Bychkov and E. I. Rashba, *J. Phys. C* **17**, 6039 (1984).

²² G. Dresselhaus, *Phys. Rev.* **100**, 580 (1955).

²³ J. Nitta, T. Akazaki, H. Takayanagi, and T. Enoki, *Phys. Rev. Lett.* **78**, 1335 (1997).

²⁴ T. Koga, J. Nitta, T. Akazaki, and H. Takayanagi, *Phys. Rev. Lett.* **89**, 046801 (2002).

²⁵ M. König, A. Tschetschelkin, E. M. Hankiewicz, J. Sinova, V. Hock, V. Daumer, M. Schäfer, C. R. Becker, H. Buhmann, and L. W. Molenkamp, *Phys. Rev. Lett.* **96**, 076804 (2006).

²⁶ T. Bergsten, T. Kobayashi, Y. Sekine, and J. Nitta, *Phys. Rev. Lett.* **97**, 196803 (2006).

²⁷ Dong Liang, and Xuan P.A. Gao, *Nano lett.* **12**, 3263 (2012).

²⁸ Y. Oreg and O. Entin-Wohlman, *Phys. Rev. B* **46**, 2393 (1992).

²⁹ D. Bercioux, M. Governale, V. Cataudella, and V. M. Ramaglia, *Phys. Rev. Lett.* **93**, 056802 (2004).

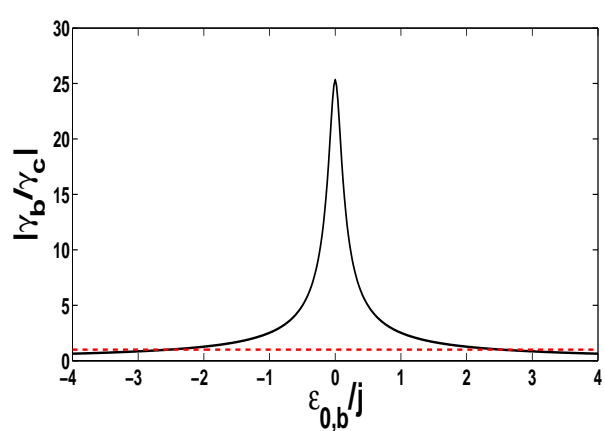
³⁰ Below we refer to ϕ as the AB flux in units of $\Phi_0/2\pi$.

³¹ A. Aharony, O. Entin-Wohlman, B. I. Halperin, and Y. Imry, *Phys. Rev. B* **66**, 115311 (2002).

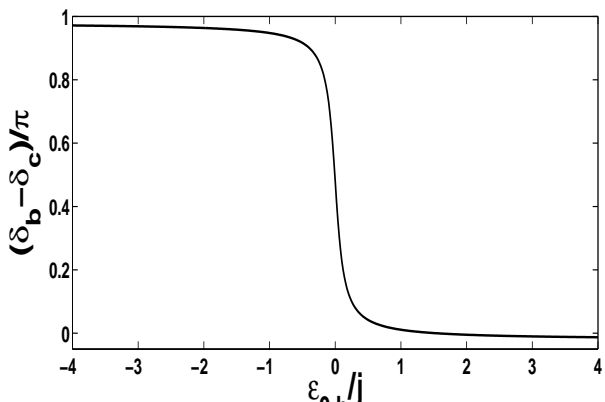
³² A. Aharony, and O. Entin-Wohlman, *J. Phys. Chem. B* **113**, 3676 (2009).

³³ We note that for $M = 1$, in which case there is no leakage to the absorbing channels, Eqs. (17) and (18) reduce to $J'_{uv} = 0$ and $J''_{uv} = J_{uv}$, respectively. In that case Eqs. (15) are identical to Eqs. (7) of Ref. 17.

³⁴ Given the spin-orbit interactions on the four edges of the diamond, one computes the SOI phase ω as follows. First one calculates the matrices U_{uv}^M . As discussed in the introduction, these matrices are of the form $U_{uv}^M = e^{i\phi_{uv} + i\mathbf{K}_{uv} \cdot \boldsymbol{\sigma}}$ with \mathbf{K}_{uv} given by Eq. (4) and ϕ_{uv} being the AB phase assigned to the edge uv (which depends on the gauge of the vector potential \mathbf{A}). From these matrices one calculates explicitly the matrix $u =$



(a)



(b)

FIG. 4: (Color online) The dependence of (a) $|\gamma_b/\gamma_c|$ and (b) $(\delta_b - \delta_c)/\pi$ (in units of π) on the site energy $\varepsilon_{0,b}$ (in units of j) for $J_{Lb} = 3j$, $J_{bR} = 4j$, $J_{Lc} = 2.5j$, $J_{cR} = 3.8j$, $J_{x,Lb} = 0.1j$, $J_{x,bR} = 0.2j$, $J_{x,Lc} = 0.05j$, $J_{x,cR} = 0.25j$, $M = 5$ and $\epsilon_{0,c} = 2j$. The dashed (red) line in (a) corresponds to $|\gamma_b/\gamma_c| = 1$.

$U_b^\dagger U_c = U_{Lb}^{-M} U_{bR}^{-M} U_{cR}^M U_{Lc}^M$. Comparing with the form $u = e^{i\phi+i\omega\hat{\sigma}} = e^{i\phi} (\cos \omega + i \sin \omega \hat{\omega} \cdot \hat{\sigma})$, one extracts the relations for $\cos \omega$, $\sin \omega$ and the blocked direction $\hat{n} = -\hat{\omega}$.